Deep gold mineralization features of Jiaojia metallogenic belt, Jiaodong gold Province: Based on the breakthrough of 3000 m exploration drilling

Xue-feng Yu, Da-peng Li, Jing-xiang Tian, De-ping Yang, Wei Shan, Ke Geng, Yu-xin Xiong, Nai-jie Chi, Peng-fei Wei, Peng-rui Liu

Citation: Xue-feng Yu, Da-peng Li, Jing-xiang Tian, De-ping Yang, Wei Shan, Ke Geng, Yu-xin Xiong, Nai-jie Chi, Peng-fei Wei, Peng-rui Liu, 2020. Deep gold mineralization features of Jiaojia metallogenic belt, Jiaodong gold Province: Based on the breakthrough of 3000 m exploration drilling, China Geology, 3, 385-401. doi: 10.31035/cg2020048.

View online: https://doi.org/10.31035/cg2020048

China Geology 3 (2020) 385−401

China Geology

Journal homepage: http://chinageology.cgs.cn
https://www.sciencedirect.com/journal/china-geology

Deep gold mineralization features of Jiaojia metallogenic belt, Jiaodong gold Province: Based on the breakthrough of 3000 m exploration drilling

Xue-feng Yu[a, b, c], Da-peng Li[a, b, c, d,*], Jing-xiang Tian[a, b, c], De-ping Yang[a, b, c], Wei Shan[a, b, c], Ke Geng[a, b, c], Yu-xin Xiong[a, b, c], Nai-jie Chi[a, b, c], Peng-fei Wei[a, b, c, d], Peng-rui Liu[a, b, c]

[a] *Shandong Institute of Geological Sciences*, *Jinan* 250013, *China*
[b] *Key Laboratory of Gold Mineralization Processes and Resources Utilization*, *Ministry of Natural Resources*, *Jinan* 250013, *China*
[c] *Key Laboratory of Geological Mineralization Processes of Metals and Resource Utilization in Shandong Province*, *Jinan* 250013, *China*
[d] *China University of Geosciences*, *Beijing* 100083, *China*

ARTICLE INFO

Article history:
Received 19 February 2020
Received in revised form 18 March 2020
Accepted 3 April 2020
Available online 28 August 2020

Keywords:
Au deposit
Alteration rock type
Fracture zone
3000 m scientific drilling
Deep mineral exploration engineering
Jiaojia metallogenic belt
Shandong Province
China

ABSTRACT

Recently, continuous breakthroughs have been made about deep gold prospecting in the Jiaodong gold province area of China. Approximately 5000 t of cumulative gold resources have been explored in Jiaodong, which has thus become an internationally noteworthy gold ore cluster. The gold exploration depth has been increased to about 2000 m from the previous <1000 m. To further explore the mineralization potential of the Jiaodong area at a depth of about 3000 m, the Shandong Institute of Geological Sciences has drilled an exploratory drillhole named "Deep drillhole ZK01" to a depth of 3266 m. Hence, as reported herein, the mineralization characteristics of the Jiaojia metallogenic belt have been successfully documented. ZK01 is, to date, the deepest borehole with an gold intersect in China, and constitutes a significant advance in deep gold prospecting in China. The findings of this study further indicate that the depth interval of 2000 m to 4000 m below the ground surface in the Wuyi Village area incorporates 912 t of inferred gold resources, while the depth interval of 2000 m to 4000 m below the surface across the Jiaodong area possesses about 4000 t of inferred gold resources. The Jiaojia Fault Belt tends to gently dip downward, having dip angles of about 25° and about 20° at vertical depths of 2000 m and 2850 m, respectively. The deep part of the Jiaojia metallogenic belt differs from the shallow and moderately deep parts about fracturing, alteration, mineralization, and tectonic type. The deep zones can generally be categorized from inside outward as cataclastic granite, granitic cataclasite, weakly beresitized granitic cataclasite, beresitized cataclasite, and gouge. These zones exhibit a gradual transitional relation or occur alternately and repeatedly. The mineralization degree of the pyritized cataclastic granite-type ore in the deep part of the Jiaojia metallogenic belt is closely related to the degree of pyrite vein development; that is, the higher the pyrite content, the wider the veins and the higher the gold grade. Compared to the shallow gold ores, the deep-seated gold ores have higher fineness and contain joseite, tetradymite, and native bismuth, suggesting that the deep gold mineralization temperature is higher and that mantle-sourced material may have contributed to this mineralization. ZK01 has also revealed that the deep-seated ore bodies in the Jiaojia metallogenic belt are principally situated above the main fracture plane (gouge) and hosted within the Linglong Granite, contradicting previous findings indicating that the moderately shallow gold ore bodies are usually hosted in the contact zone between the Linglong Granite and Jiaodong Group or meta-gabbro. These new discoveries are particularly significant because they can help correct mineralization prospecting models, determine favorable positions for deep prospecting, and improve metallogenic prediction and resource potential evaluation.

1. Introduction

Recently, about 5000 t of accumulative gold resource reserves were identified in Jiaodong (Yu XF et al., 2018a), which has since become an internationally noteworthy gold ore concentration area. The large-scale, short-duration, and high-intensity mineralization events that occurred in Jiaodong have attracted both domestic and international scientists, and extensive in-depth geological scientific research has been conducted. This research has mainly involved regional tectonic setting of the gold mineralization processes (Groves

First author: *E-mail address*: xfengy@sohu.com (Xue-feng Yu)..
* Corresponding author: *E-mail address*: dpengli@126.com (Da-peng Li).

doi:10.31035/cg2020048
2096-5192/© 2020 China Geology Editorial Office.

DI et al., 1998; Goldfarb RJ et al., 2001; Chen YJ et al., 2004; Deng J et al., 2006; Jiang SY et al., 2009; Goldfarb RJ and Santosh M, 2014; Yu XF et al., 2018a, 2018b; Mao XC et al., 2019; Yang LQ et al., 2019), magma evolution mechanisms (Yang JH et al., 2003; Mao JW et al., 2005; Pirajno F and Santosh M, 2014; Yang LQ et al., 2018; Dou JZ et al., 2018), ore-forming fluids (Fan HR et al., 2005; Mao JW et al., 2005; Zhai MG and Santosh M, 2013; Chai P et al., 2019; Li J et al., 2020a), mineralization (Groves DI et al., 1998; Zhai MG et al., 2004; Fan HR et al., 2005; Deng J et al., 2006; Goldfarb RJ and Santosh M, 2014; Yang LQ et al., 2014, 2016, 2017; Yu XF et al., 2015, 2016; Li J et al., 2016; Han ZY et al., 2019; Liu XD et al., 2019), and the ore-forming mechanisms (Kerrich R et al., 2000; Goldfarb RJ et al., 2001, 2014; Zhai MG and Santosh M, 2013; Li SR and Santosh M, 2014; Zaw K et al., 2014; Ma L et al., 2016; Guo LN et al., 2016; Cai YC et al., 2018; Liu C et al., 2018; Li Q et al., 2019; Shan W et al., 2019) and age (Goldfarb RJ et al., 2001; Chen YJ et al., 2004; Yu XF et al., 2015; Ding ZJ et al., 2015; Zhu BL et al., 2016; Song MC et al., 2017; Yao XF et al., 2019; Sai SX et al., 2020; Li J et al., 2020b).

Since 2011, continuous and significant breakthroughs have been made about deep prospecting of large gold belts such as those at Sanshandao, Jiaojia, and Zhaoping in Jiaodong, which hold about 3000 t of additional resources (Hao ZG et al., 2016; Wang JH and Tian JX, 2017; Yu XF et al., 2018a; Editorial Department of China Geology, 2018; Wang J et al., 2019). The Sanshandao, Jiaojia, and Linglong-Dayingezhuang gold fields have been recognized as globally significant gold fields with reserves exceeding thousands of tons. Furthermore, the Zhaoyuan-Laizhou ore concentration area is now considered to be the world's third-largest gold deposit (with more than 4000 t of accumulative reserves) (Yu XF et al., 2018a, 2018b). Recently, a mineralized zone characterized by beresitization and potassic-altered granite has been discovered at a depth of about 2200 m in the deep part of the Jiaojia Fault Belt (characterized by a deep drillhole of 2200 m depth in the Shaling Mine). Although the individual ore bodies are not large in scale, they have experienced intense mineralization and alteration processes and the large-scale structures are complex. In the developed ore-hosting spaces, the ore bodies are small but large in number. The ore bodies may be much more complex than theoretical models suggest. Regardless, the gold resources in the deep part of the Jiaojia metallogenic belt undoubtedly have significant prospecting potential. However, many questions remain. For instance, it is unclear whether gold ore bodies occur in the deeper part of the Jiaojia Fault Belt, and whether their alteration and mineralization characteristics are consistent with those of the shallow enrichment belt. The vertical variations of the properties of the main controlling fault are also unknown. These questions emphasize the importance of ultradeep (2000 m to 3000 m deep) prospecting and scientific research in the Jiaojia metallogenic belt. Besides, research on the geological characteristics, mineralization, metallogenic regularities, and resource potential of the deep part of the Jiaodong area, as well as the promotion of major projects related to deep earth resource exploration, are exceptionally important.

The Shandong Institute of Geological Sciences has created a 3266 m scientific drillhole named "Deep drillhole ZK01" in 2016 in the Jiaojia Fault Belt at Wuyi Village, Laizhou City. This drillhole is the first deep exploration drillhole in the Jiaojia metallogenic belt as well as China's first deep drillhole with intersected hard-rock gold mineralization and constitutes a significant advance in deep-gold exploration in China.

The present study reports the successful definition of the gold ore bodies in the deep part of the Jiaojia Fault Belt based on samples obtained via ZK01. Hence, the gold mineralization characteristics of the deep part of the Jiaojia metallogenic belt (at 3000 m) that intersects a new gold layer are revealed and first-hand data on the deep part of the Jiaojia metallogenic belt are reported. The implications of these characteristics are also discussed.

2. Geological setting

The Jiaodong Peninsula is located in the southeastern portion of the North China Craton and the western margin of the Pacific Plate. The Jiaodong Peninsula is bordered by the Tancheng-Lujiang Fault belt to the west and the Dabie-Sulu ultrahigh-pressure metamorphic belt to the southeast. This peninsula is principally composed of Pre-Cambrian basement rocks and has undergone Mesozoic tectonic-magmatism (Fig. 1). The Neoarchean Qixia Sequence is the most widespread metamorphosed pluton in the study area and generally spreads WE. It is mainly composed of tonalite, trondhjemite, and granodiorite. The island-shaped Neoarchean Jiaodong Group and Malianzhuang Sequence residual are included in Qixia Sequence. Jiaodong Group primarily comprises amphibolite and biotite granulite, which constitute a set of regional metamorphic rocks of amphibolite and amphibolite-granulite facies. Malianzhuang Sequence is mainly composed of meta-gabbro. Paleoproterozoic Fenzishan and Jingshan Group are younger khondalite series, which comprises two mica schist, graphite schist, marble, diopside granulite, and plagioclase amphibolite. In the past, intense and frequent magma intrusion occurred within the Jiaodong area. Thus, the Mesozoic intrusive rocks are mainly composed of 165–150 Ma Linglong Sequence *in situ* remelting-type calc alkaline biotite adamellite and 132–123 Ma Guojialing Sequence crust-mantle mixing (Yang KF et al., 2012; Deng J et al., 2015), as well as 120−110 Ma Weideshan Sequence high-K calcalkalic porphyritic-like granodiorites (Hou ML et al., 2007; Yang KF et al., 2012). Besides, natural dykes composed of materials such as lamprophyre, dioritic porphyrite, and diabase porphyrite have developed. The ore-controlling structures within the area primarily include the Sanshandao and Jiaojia faults, the shallow parts of which extend NNE-NE along with the Linglong Sequence granite with Jiaodong Group metamorphic rocks (Wang LG et al., 1998; Goldfarb RJ et al., 2014). In the past, Northwestern Jiaodong underwent intense craton destruction and continental arc tectonic-magma reworking. In particular, the gold deposit formation that occurred within the Jiaodong area has

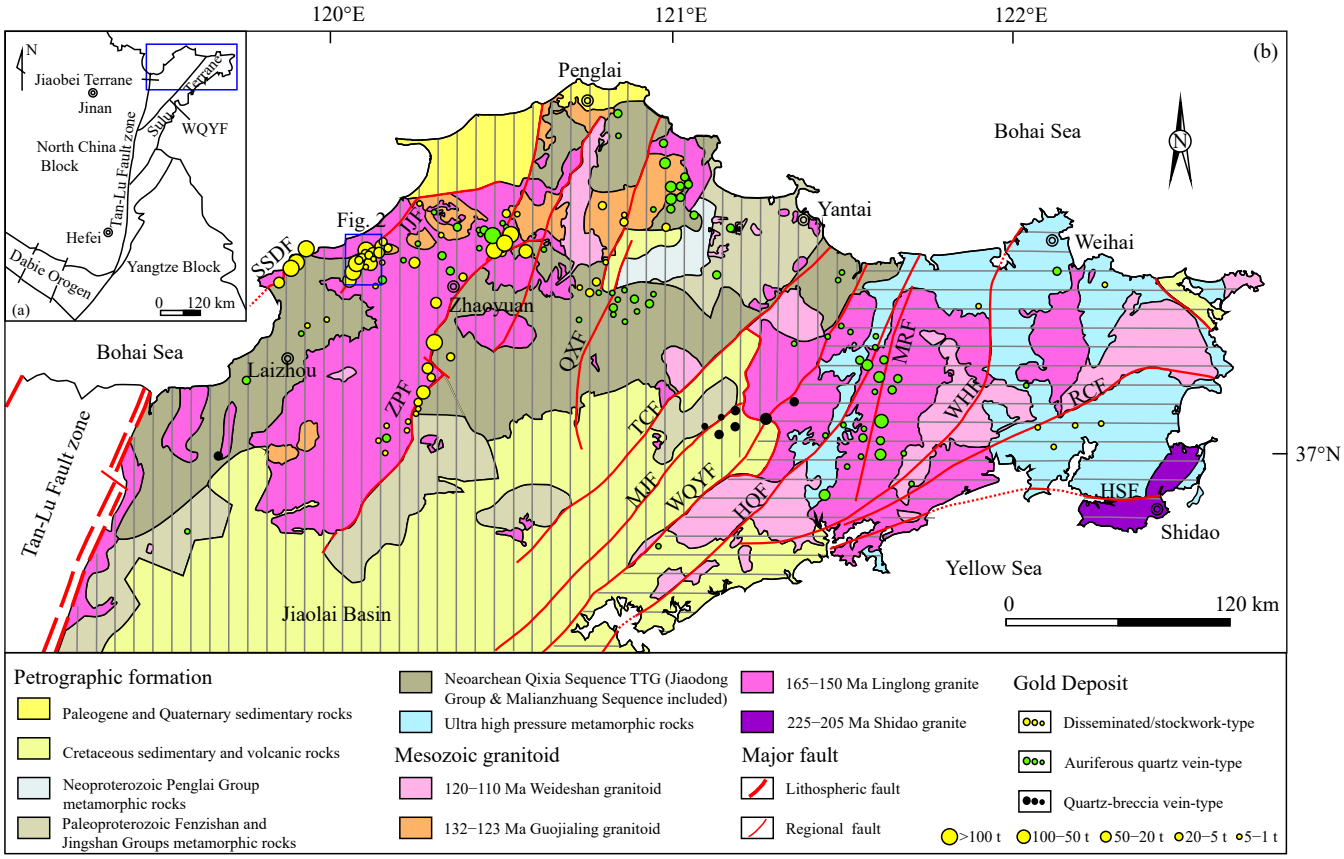

Fig. 1. Regional geological sketch of the Jiaodong Peninsula (modified from Yang LQ et al. 2014). HQF–Haiyang-Qingdao Fault; HSF–Haiyang-Shidao Fault; JJF –Jiaojia Fault; MJF –Muping-Jimo Fault; MRF –Muping-Rushan Fault; QXF –Qixia Fault; RCF –Rongcheng Fault; SSDF–Sanshandao Fault; TCF–Taocun Fault; WHF–Weihai Fault; WQYF–Wulian-Qingdao-Yantai Fault; ZPF–Zhaoping Fault.

generally been considered to be closely related to Mesozoic tectonic-magmatic hydrothermal activity or collisional orogeny (Mao JW et al., 2005, 2008; Yang LQ et al., 2014; Goldfarb RJ and Santosh M, 2014; Yang QY et al., 2013). Extensive mineralization is also thought to have contributed, occurring at 130–110 Ma (Late Middle Mesozoic) (Chen YJ et al., 2004; Yu XF et al., 2018b) under a setting of large-scale lithosphere thinning, with a transition from compressive to extensional occurring during Mesozoic oceanic crust subduction or continental-continental collisional orogeny (Chen YJ et al., 2004; Mao JW et al., 2008; Jiang SY et al., 2009; Goldfarb RJ and Santosh M, 2014; Yang QY et al., 2013).

The Jiaojia Fault is a metallogenic structural belt having the most densely developed gold deposits in northwestern Jiaodong. This fault belt is generally divided into three segments at the surface from north to south: The Sizhuang, Matang-Xincheng, and Xincheng-Gaojiazhuangzi segments. The fault extends to about 60 km, with strikes of 35°–40° and dips of 30°–50°, along with local dips of 80°. Its maximum thickness is up to 1000 m. As it is separated by the main fracture plane, the alteration zone appear to display symmetrical zoning. The gold ore bodies in the shallow part of the Jiaojia Fault Belt (above −1500 m) are mainly hosted in the highly altered rocks of the hanging wall below the main fracture plane and are characterized by disseminated or veinlet-disseminated mineralization. In recent years, large gold deposits in the depth of Sizhuan and Jiaojia, as well as in the shallow of Zhuguolijia, Nanlü-Xinmu, Shaling, and Qianchen deposits have been successively discovered in the central-southern segment of the Jiaojia Fault, and about 800 t of additional gold reserves have been identified in the Jiaojia metallogenic belt. To date, about 1400 t of accumulative gold resource reserves have been identified. The main ore body of the Shaling gold mine in Laizhou has a controlled length of up to 1920 m, a maximum along-dip depth of 2180 m, and an elevation of −940 m to −2020 m. Further, 389 t of gold resources have been identified in the mine at an average grade of 3.41×10^{-6} gold. The low-grade gold resources total 61 t, with an average grade of 1.44×10^{-6} gold and an average ore-body thickness of 6.8 m (Yu XF et al., 2016). The main ore bodies of the shallow deposits in the Jiaojia metallogenic belt usually connect as one in the depth direction, before pitching outward and reoccurring along the strike and dip. The mineralization dynamics of the gold deposits have unique characteristics compared to other international large-scale gold deposits, and elucidation of the sources and enrichment mechanisms of the super-large amounts of gold is of considerable scientific importance.

3. Structures of geological bodies in the deep part of Jiaojia metallogenic belt

ZK01 has revealed that the Jiaojia Fault Belt dips more

gently toward the deep part and is an upper-steep and lower-gentle shovel-like fault, dipping at about 25° and about 20° at vertical depths of 2000 m and 2850 m, respectively. The belt thickness increases from about 500 m in the shallow portion to more than 800 m in the depth direction, where the mineralized alteration becomes more complex. From the margin toward the center, the degree of fracturing and alteration first increases and then alternates between increasing and decreasing. The belt zoning becomes complex, transitioning from simple and symmetric to asymmetric (Fig. 2). The main geological bodies from the lower range upward are mainly Quaternary, Xinzhuang-Unit tonalitic gneiss of the Qixia Sequence and Luanjiazhai-Unit plagioclase amphibolite of the Malianzhuang Sequence, Cuizhao-Unit biotite monzonitic granite of the Linglong Sequence, beresitized granitic cataclasite, cataclastic adamellite (the horizon-hosting main ore bodies), gouge and tectonic breccia, beresitized cataclastic biotite-adamellite, and adamellite of the Linglong Sequence (Fig. 3). The deep tectonic breccias of the fault belt comprise mylonite and cataclasite dominated by ductile and brittle deformation, respectively. The former developed in the early faulting stage and are usually covered by mineralization and alteration. Brittle deformation occurring via multiple cataclastic processes is evident, which caused formation of cataclastic granite or granitic cataclasite; this observation coincides with findings from the shallow part of the Jiaojia Fault. Previous research has indicated that the Jiaojia Fault exhibits multiple activity characteristics, and researchers generally believe that this fault experienced sinistral compress shear activity causing mylonite formation. The faulting indicates dextral transtensional or trans-shearing (Wang JC et al., 2003; Miao LC et al., 1997; Li HM et al., 2002; Li JJ et al., 2005; Zhao ZL, 2016) providing space for ore-forming fluid migration and precipitation. The post-mineralization fault is dominated by compression with transpression (Song MC et al., 2010; Yu XF et al., 2018b).

According to sample data collected from ZK01, the characteristics of the main rock formations from the surface downward are as follows.

(1) 0–28.70 m: Linyi-Formation pebbled loam and loam of Quaternary.

(2) 28.70–1321.84 m: Xinzhuang-Unit tonalitic gneiss of the Qixia-Sequence and Luanjiazhai-Unit plagioclase amphibolite (meta-gabbro) of the Malianzhuang Sequence (Fig. 3a). The tonalitic gneiss is off-dark gray to grayish-green in color and gneissic with a nematoblastic-granoblastic texture. Jiaodong-Group amphibolite and hornblende enclaves have developed in this rock. The plagioclase amphibolite is off-dark gray to dark-black to grayish-green in color and has weakly gneissic, striped-banded, and massive structures, with a nematoblastic-granoblastic texture. Garnet phenocrysts and minor epidote, carbonate, and pyrite are locally observable. In the rock, Jiaodong-Group biotite granulite, biotite monzogranulite, and amphibole-plagioclase granulite enclaves

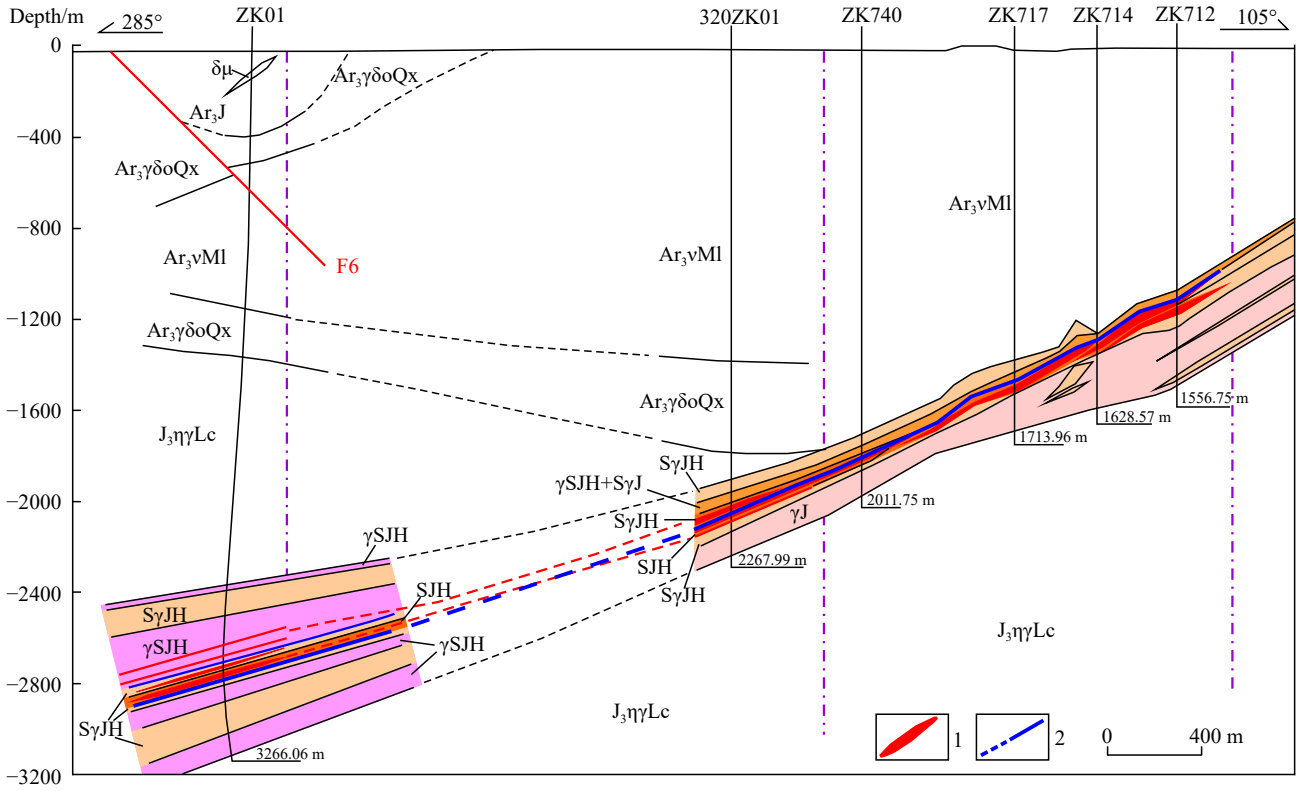

Fig. 2. Section of Jiaojia fractured-alteration belt based on deep drilling. Ar_3J–Jiaodong Group plagioclase amphibolite, biotite monzogranite, and biotite-amphibole granulite; $Ar_3γδoQx$–Xinzhuang-Unit tonalitic gneiss of Qixia Sequence; $Ar_3νMl$–Luanjiazhai-Unit of Malianzhuang Sequence; $J_3ηγ$ Lc–Cuizhao-Unit biotite adamellite of Linglong Sequence; γJ–phyllic granite; γJH–beresitized granite; γSJH–beresitized cataclastic granite; SγJ–phyllic granitic cataclasite; SγJH–beresitized granitic cataclasite; SJH–beresitized cataclasite; δμ–diorite porphyrite; 1–gold ore body; 2–main fracture plane (gouge).

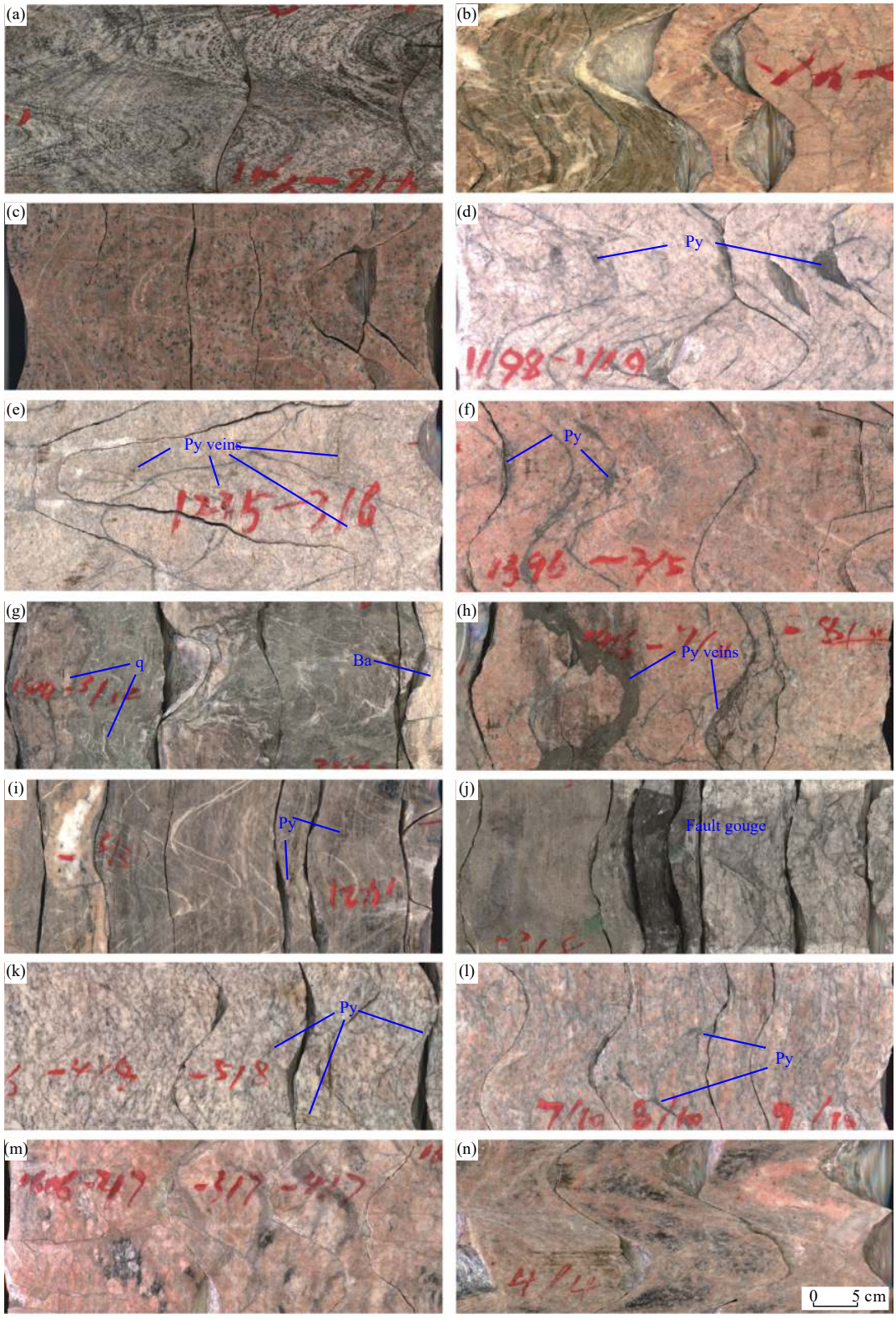

Fig. 3. Scanned photographs showing the ZK01 drillhole core. All photographs were taken using a core scanner and present core surface development. The photograph width is the core perimeter (188.40 mm). All photographs have the same scale. Detailed discription of each layer is given in the text.

are common. Luanjiazhai-Unit plagioclase amphibolite is crosscut by tonalitic gneiss at depth intervals of 520.54 m to 1174.74 m and 1027.74 m to 1079.94 m.

(3) 1321.84–1390.94 m: Contact between Qixia-Sequence tonalitic gneiss and Cuizhao-Unit biotite adamellite of the Linglong Sequence (Fig. 3b). In the upper depth interval of 1321.84 m to 1381.74 m, mylonitized felsic altered rocks and intensely sericitized, carbonatized tonalitic mylonites are apparent with intense alteration and developed quartz veins, along with disseminated pyrite and chalcopyrite. In the lower

depth interval of 1381.74 m to 1390.94 m, cataclastic granite with carbonatization and sericitization are apparent, along with minor pyrite.

(4) 1390.94–2416.29 m: Cuizhao-Unit biotite-adamellite of the Late Yanshanian Linglong Sequence (Fig. 3c). This rock type is off-flesh pink, massive with a granitic texture, and relatively broken with developed fissures. Some of the rocks exhibit characteristics such as kaolinization, chloritization, silification, sericitization, and carbonatization, with disseminated and veinlet-like pyrite. In the lower depth interval of 1755.94 m to 2416.29 m, cataclastic biotite-adamellite with potash alteration and silification is apparent. Potash alteration has typically occurred along fissures, being associated with pyrite or sericite.

(5) 2416.29–2466.44 m: An upper branch of the Jiaojia Fault Belt mainly containing beresitized cataclastic adamellite (Fig. 3d), which is off-shallow flesh pink to shallow gray, with blastogranitic and cataclastic structures. The altered minerals include sericite, carbonate minerals, and pyrite. The pyrites are disseminated or veinlet-like, stockwork, and lumpy along the fissures. Further, some pyrite veinlets are crosscut by late-stage quartz-carbonate veins. In several samples, native gold can be observed in vein-like pyrite-filled fissures.

(6) 2466.44–2549.59 m: Beresitized granitic cataclasite (Fig. 3e) with an off-shallow grayish-white to shallow flesh pink color and broken with developed fissures having a cataclastic texture. Developed carbonatization, pyritization, and sericitization are apparent. The pyrites are disseminated, veinlet-like, and locally lumpy. The pyrite veinlets are crosscut, indicating pyrites in a multi-phase development.

(7) 2549.59–2801.34 m: Beresitized granitic cataclasite and cataclastic adamellite (Fig. 3f), colored off-shallow grayish-white to shallow flesh pink and broken and massive with cataclastic and blastogranitic structures. The main alteration types are sericitization, silification, and carbonatization. The main metal minerals are pyrite, chalcopyrite, galena, gold minerals, and pyrrhotite. The pyrites are vein-like, lumpy, spotted, or disseminated, and xenomorphic-subhedral granular, with grain sizes generally within 0.05−0.5 mm. Galena occurs in the form of anhedral micro-grains included in pyrites. Chalcopyrites are distributed among the quartz grains. This layer contains two gold ore bodies and is of cataclastic adamellite ore type. The two ore bodies have thicknesses of 0.85 m and 1.67 m and average grades of 3.21×10^{-6} and 1.77×10^{-6} gold, respectively.

(8) 2801.34–2801.58 m: Fault gouge and tectonic breccia, constituting the first fault gouge layer. The rock is colored off-grayish green to dark green, with a layered structure, and is about 5 cm thick. The tectonic breccia is composed mainly of quartz, with a grain size of about 1 cm.

(9) 2801.58–2810.89 m: Pyrite-bearing Cr-sericitized altered rock (Fig. 3g). The rock is off-grayish green with local viridian, which is typical in color; massive with a flaky granoblastic texture; and mainly composed of carbonate minerals, quartz, sericite, and muscovite (Fig. 4c). The carbonate minerals, affected by stress, exhibit fracturing, and wavy extinction superimposed with late-stage phyllic alteration. The sericite and muscovite are off-viridian colored because they contain Cr, and are crosscut with carbonate veinlets and barite veins. Note that this rock type is also observable in shallow drill holes in the Jiaojia metallogenic belt, but these deposits are relatively thin, generally being 10–40 cm thick.

(10) 2810.89–2824.39 m: Beresitized cataclastic biotite-adamellite (Fig. 3h). The rock is colored off-shallow flesh pink to shallow grayish-green, with blastogranitic and cataclastic structures. The altered minerals include sericite, pyrite, and carbonate minerals. The pyrites are enriched and mostly occur as stockworks. A gold ore body of 5.00 m thickness has been discovered, having average and maximum grades of 3.13×10^{-6} and 13.65×10^{-6} gold, respectively.

(11) 2824.39–2854.59 m: Beresitized rock and beresitized granitic cataclasite (Fig. 3i). The rock is grayish black with irregular fissures and shows weak orientation and mylonitization. The rock is massive with lepidogranoblastic and cataclastic structures. The altered minerals include sericite, quartz, and pyrite. The pyrites are disseminated and vein-like, and the vein-like pyrites are usually associated with quartz veins. Late-stage carbonate veins are also observable. The mylonitic texture formed by early-stage ductile deformation is usually covered by late-stage brittle faults and beresitization. This layer has the strongest alteration and mineralization, and three gold ore bodies have been discovered in this location. The ore types include beresitized granitic cataclasite and beresitized cataclasite. The three ore bodies have thicknesses of 3.32 m, 5.77 m, and 4.26 m at average grades of 1.48×10^{-6}, 1.08×10^{-6}, and 1.37×10^{-6} gold, respectively.

The characteristics described above correspond to the traditional hanging wall of the Jiaojia Fault fractured belt.

(12) 2854.59–2854.69 m: Fault gouge (the second fault gouge layer, main fracture plane) (Fig. 3j), colored off-black to shallow-green. Dark-black and shallow-green fault gouges exist, both being 5 cm thick, with a schistosity texture and an axis angle of 75° coinciding with the fault belt attitude. This interval is loose and broken and corresponds to the main fracture plane of the Jiaojia Fractured Belt. The fault gouge layer is thin but extends stably and is almost observable and traceable in all shallow drillholes that penetrate the Jiaojia metallogenic belt.

(13) 2854.69–2876.89 m: Beresitized granitic cataclasite (Fig. 3k) colored off-shallow flesh pink to grayish-white, which is massive with lepidogranoblastic, weakly mylonitic, and cataclastic structures. The altered minerals are mainly sericite, pyrite, quartz, and carbonate minerals. The rock is crosscut by black networked quartz-pyrite veins and beresitized rock veinlets.

(14) 2876.89–2965.79 m: Beresitized cataclastic adamellite intercalated with beresitized granitic cataclasite (Fig. 3l).

(15) 2965.79–3111.93 m: Beresitized granitic porphyroclastic rock and granulitic rock.

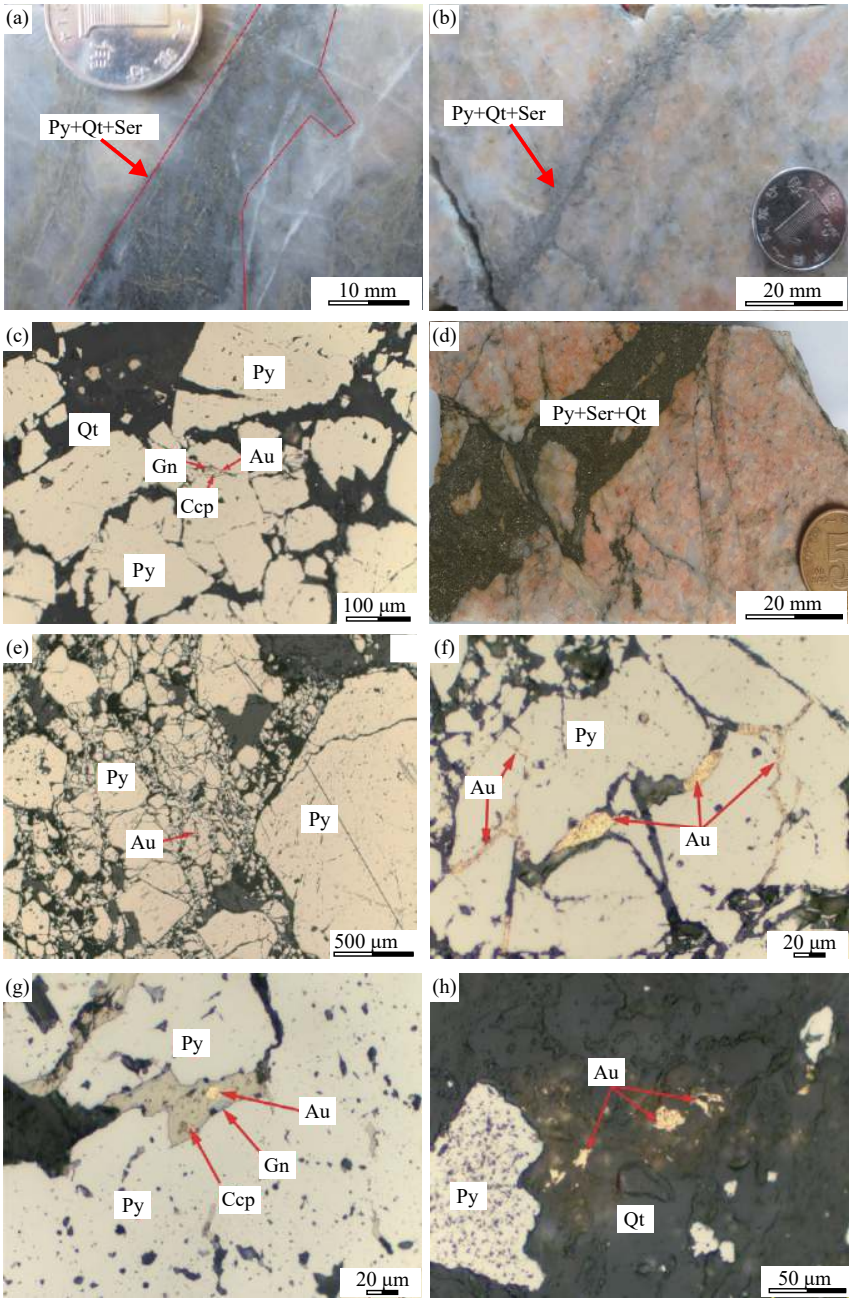

Fig. 4. Characteristics of ores in the deep part of Jiaojia metallogenic belt. a, b, d−core section; c, e, f, g, h−under microscope. Detailed description of each layer is given in the text. Ccp−Chalcopyrite. Py−Pyrite; Qt−Quartz; Ser−Sericite; Gn−Galena; Au−gold mineral.

(16) 3111.93–3234.16 m: Weakly beresitized cataclastic biotite-adamellite (Fig. 3m). The rock is colored off-shallow grayish-white to shallow gray, with developed fissures. The fissures are filled with pyrites and silification is apparent. This layer corresponds to the bottom of the Jiaojia metallogenic belt based on deep drilling.

(17) 3234.16–3266.06 m: Cataclastic porphyroid adamellite (Fig. 3n). The rock is colored off-shallow flesh pink to shallow grayish-white, being massive with cataclastic and blastogranitic structures. No sulfide or mineralization is apparent. In this layer, a typical porphyroid texture is observable and the protolith may be different from the upper biotite-adamellite.

4. Characteristics of deep-seated gold ore bodies of Jiaojia metallogenic belt

4.1. Characteristics of deep-seated gold ore bodies

From the acquired ZK01 data, the Jiaojia Fault Belt was characterized at a depth interval of 2416.29 m to 3234.16 m, and six gold ore bodies were discovered at a depth interval of 2700.89 m to 2854.59 m (Table 1). These ore bodies are located at elevations of −2846.22 m to −2692.52 m and have a total thickness of 20.87 m and average and maximum grades of 1.85×10^{-6} and 13.65×10^{-6} gold, respectively. Ore bodies display quasi-lamella and lenticular in shapes, with a NS-striking, inclined toward the W at 20° dip angle. The ore

bodies Ⅰ-1 and Ⅰ-3 are industrial ore bodies with a thickness of 5.85 m and the average grade of 3.14×10^{-6} gold. The natural ore type is beresitized cataclastic granite. Also, six layers of mineralized bodies with a total apparent thickness of 11.00 m have been delineated in the deep part of the Jiaojia Fault Belt; the mineralization types are mainly beresitized granitic, beresitized, and granitic cataclasite.

The ore types in the deep part of the Jiaojia metallogenic belt are similar to those in the central-shallow part, and the industrial ore type classification is low-S gold ore. The deposits in the belt are fractured alteration gold deposits, i.e., Jiaojia-type gold deposits. According to the fractured alteration intensity and main structural characteristics, the ore types can be divided into the following two categories: (1) Beresitized cataclasite and (2) beresitized cataclastic granite. (1) For the beresitized cataclasite (Fig. 4a), the ore is off-grayish green to grayish-black in color and mainly occurs in the center of the alteration zone. Uneven fractured alteration is apparent and some of the ore has a residual granite appearance (Fig. 4b). The ore exhibits lepidogranoblastic and porphyroclastic structures and massive, veinlet-disseminated, and densely disseminated structures. Disseminated pyrite, together with quartz and sericite, forms veinlets and stockworks that fill the rock fissures, constituting a veinlet-disseminated structure. The dominant metal minerals are pyrite, with minor chalcopyrite, galena, sphalerite, and gangue mineral deposits dominated by feldspar, quartz, and sericite, along with minor carbonate mineral deposits (Fig. 4c). (2) As regards the beresitized cataclastic granite (Fig. 4d), the ore is off-flesh pink to grayish-white in color and occurs in cataclastic adamellite having clear characteristics, including a blastogranitic texture. Pyrite or beresite veins are relatively developed, with a highly variable gold grade. High-grade ore is observable. The dominant metal minerals are pyrite, with occasional chalcopyrite (Fig. 4e), and gangue minerals dominated by feldspar and quartz with minor sericite and chlorite.

4.2. Ore mineral characteristics

The minerals associated with the deep-seated ores are divided into three types: (1) Residual minerals from protolith, such as plagioclase, K-feldspar, quartz, and biotite; (2) altered non-metallic minerals, including sericite, micro-grained quartz, K-feldspar, carbonate minerals, chlorite, and kaolinte; (3) metal minerals, including pyrite, galena, chalcopyrite, sphalerite, pyrrhotite, natural gold, and electrum, occasionally with local joseite and native bismuth.

The natural gold are mainly distributed in pyrite and crystal fissures (Fig. 4f) or interlocked with chalcopyrite and galena in pyrite and crystal fissures (Fig. 4g). Furthermore, minor gold minerals are apparent in quartz grains (Fig. 4h). The gold minerals principally have grain sizes of 1–70 μm, being dominated by gold micro-particles (47.59%) and fine-grained gold (43.67%), with minor medium-grained gold (6.02%) and coarse-grained gold (2.71%). Furthermore, in this study, <1 μm wide gold lines and <0.02 μm gold submicro-grains were observed using a scanning electron microscope. Pyrite is a predominant gold carrier. Early-stage pyrites usually occur as euhedral−subhedral grains disseminated in granite and are mostly distributed along the granite gneissosity. It is apparent that the late-stage pyrites mostly developed along rock fissures, forming pyrite-quartz veinlets or beresite veins. Furthermore, the pyrites that formed during variable mineralization stages differ from each other. That is, the pyrites in the quartz-pyrite and gold-beresite stages are mostly found in the form of irregular grains having an off-shallow yellow color, with strong metal luster and exhibiting cataclasis. The coarser pyrite grains tend to appear in vein-like aggregates with quartz. Further, the pyrites formed in the gold-beresitization stage are dominated by fractured, fine, small-sized grain aggregates, usually occurring as veinlets, stockworks, and dense disseminations. The pyrites of the gold-quartz-polymetallic sulfide stage are dominated by fine-grained euhedral crystals and are off-grayish yellow in color with a dark luster; and these pyrites usually occur with chalcopyrite, galena, and sphalerite in the form of veinlets and stockworks. Chalcopyrites mostly occur as allotriomorphic grains among pyrite grains, being locally distributed among quartz grains with grain sizes generally between 0.02 mm and 0.2 mm. The chalcopyrites formed at a later stage than the pyrites and are usually interlocked with galena or distributed in beresite veins.

To investigate the useful and harmful components of the ore, excluding gold, deep ore composites were analyzed. Composite samples from different ore bodies were combined according to ore type, based on sample length ratio and using analysis duplicates. Seven composite samples were collected for analysis. The basic and composite analyses of the ore indicated that the useful components are dominated by gold

Table 1. List of deep-seated ore bodies of Jiaojia metallogenic belt.

Ore body ID	Burial depth/m	Apparent thickness /m	True thickness /m	Average grade /10^{-6}	Maximum grade /10^{-6}	Ore type
Ⅰ-1	2700.89−2701.89	1.0	0.85	3.21	3.21	Beresitized cataclastic granite
Ⅰ-2	2777.89−2779.89	2.0	1.67	1.77	2.22	
Ⅰ-3	2813.89−2819.89	6.0	5.00	3.13	13.65	
Ⅰ-4	2828.39−2832.39	4.0	3.32	1.48	3.34	Pyrite phyllic-altered granitic cataclasite
Ⅰ-5	2838.39−2845.39	7.0	5.77	1.08	2.07	
Ⅰ-6	2849.39−2854.59	5.2	4.26	1.37	1.82	Beresitized cataclasite (porphyroclastic, granulitic, and crushed-powder rocks)

and the associated components are dominated by Ag and S, which can be comprehensively recycled and utilized. The other component fractions are low and similar to those in medium-shallow ore bodies (Table 2).

Electron probe analyses (JEOL, JXA8230) of the gold minerals in the main ore types (Table 3) revealed high gold fineness in the deep ores of the Jiaojia metallogenic belt. Further, the gold minerals mostly have >80% gold content, with minor cases of ≦80%, in the form of native gold with subordinate electrum and minor contents of Fe, Bi, Zn, Cu, S, As, Sb, and Te. The gold fineness varies from 771 to 909. Compared to the shallow deposits, the deep-seated deposits display significantly higher gold fineness.

5. Alteration and mineralization of the deep part of Jiaojia metallogenic belt

5.1. Alteration types and zoning

Previous research has indicated that the alteration zoning of the shallow part of the Jiaojia metallogenic belt is generally beresite-centered with outward beresitized granulitic rock, beresitized granitic porphyroclastic rock, and phyllic cataclastic granite (Shenyang Institute of Geology and Mineral Resources, 1988). Various zones are in transition. Furthermore, an ordered fault belt structure that formed during development of the fault belt is apparent, having typical zoning; the main fracture plane, gouge, compressive schistosity, tectonic lens, dense joint, and sparse joint zones are located from the fault center outward (Deng J et al., 1996). These findings indicate that the alteration zoning of the deep part of the Jiaojia metallogenic belt differs significantly from that of the shallow part. According to the rock mineralization and alteration intensity, the type of mineralization and alteration, and the fracturing intensity, the deep part of the Jiaojia metallogenic belt (2416.29–3234.16 m) can be broadly divided into 12 lithological layers. Separated by the black fault gouge, the hanging wall contains seven layers while the footwall contains four layers (Table 4). The various layers are in gradual transition. Along the main fracture plane outward, there is a gradual decrease in fracturing intensity and pyritization, beresitization, and silicification. Further, the mineralization and alteration transition from dense veinlets and densely disseminated beresitization to veinlet and

Table 2. Composite analysis results for Jiaojia metallogenic belt deep ores.

Composite ID	Ore body ID	Ore type	Ag/10^{-6}	Cu/10^{-2}	Pb/10^{-2}	Zn/10^{-2}	S/10^{-2}	As/10^{-6}
ZH1	Ⅰ-1	(1)	1.6	0.013	0.003	0.003	2.88	10.47
ZH2	Ⅰ-2	(1)	1.1	0.006	0.005	0.003	1.15	6.59
ZH3	Ⅰ-3	(1)	2.0	0.002	0.002	0.004	1.93	3.07
ZH4	Ⅰ-4	(2)	1.5	0.004	0.002	0.004	0.32	1.30
ZH5	Ⅰ-5	(2)	＜1.0	0.010	0.003	0.007	1.12	6.18
ZH6	Ⅰ-6	(3)	1.3	0.001	0.022	0.061	1.42	10.60
ZH7	Mineralized layer		＜1.0	0.001	0.001	0.002	1.86	4.20

Notes: Ore types: 1–beresitized cataclastic granite; 2–beresitized granitic cataclasite; 3–beresitized cataclasite (porphyroclastic, granulitic, crushed-powdered). These analyses were performed at the Jinan Mineral Resources Monitoring and Testing Center of the former Ministry of Land and Resources. Methodology: Atomic absorption spectrophotometry (Perkin Elmer, PE-400).

Table 3. Electron probe analysis results for gold minerals in the deep part of Jiaojia metallogenic belt (ω_B/%).

Sample ID	Au	Ag	Cu	Pb	Zn	Fe	As	Sb	Bi	S	Te	Total	Name
g35-1	89.07	8.43	0.00	0.00	0.00	0.37	0.00	0.00	0.84	0.00	0.00	98.70	Native gold
g35-2	87.27	9.38	0.02	0.00	0.00	1.09	0.05	0.00	0.78	0.05	0.04	98.68	Native gold
g35-3	88.75	8.11	0.00	0.00	0.00	1.57	0.03	0.00	0.57	0.09	0.00	99.12	Native gold
g37-1	80.02	16.14	0.06	0.00	1.41	0.00	0.00	0.72	0.00	0.07	0.00	98.43	Native gold
g37-2	79.10	17.86	0.46	0.00	0.00	3.13	0.01	0.01	0.66	0.19	0.02	101.44	Native gold
g37-3	77.90	18.94	0.02	0.00	0.00	2.78	0.00	0.00	0.61	0.65	0.11	101.00	Native gold
g37-4	79.98	17.95	0.08	0.00	0.00	2.28	0.00	0.00	0.62	0.14	0.06	101.10	Native gold
g45-1	85.13	11.28	0.01	0.00	0.00	2.99	0.00	0.00	0.60	0.03	0.21	100.25	Native gold
g45-2	88.01	7.41	0.00	0.00	1.36	0.00	0.03	0.77	0.00	0.09	0.00	97.67	Native gold
g45-3	90.20	6.58	0.01	0.00	1.48	0.00	0.00	0.63	0.01	0.28	0.00	99.19	Native gold
g45-4	86.37	10.82	0.00	0.00	2.89	0.00	0.00	0.62	0.01	0.74	0.00	101.45	Native gold
g61-1	86.97	10.07	0.07	0.00	0.03	0.80	0.00	0.00	0.78	0.04	0.03	98.79	Native gold
g61-2	87.39	10.47	0.00	0.00	0.02	0.77	0.00	0.00	0.81	0.05	0.03	99.54	Native gold
g61-3	86.19	11.00	0.00	0.00	0.00	1.24	0.00	0.00	0.72	0.09	0.04	99.29	Native gold
g61-4	86.30	10.24	0.00	0.00	0.04	1.04	0.02	0.00	0.73	0.13	0.03	98.53	Native gold
g61-5	86.68	10.77	0.01	0.00	0.00	1.68	0.01	0.00	0.81	0.15	0.03	100.14	Native gold

Notes: These analyses were conducted at the Jinan Mineral Resources Monitoring and Testing Center of the former Ministry of Land and Resources. Test equipment: Electron probe (JEOL, JXA8230). Test conditions: Accelerating voltage, 15 kV; probe electric current, 2×10^{-8} A; spot size, 10 μm. Standards used were natural minerals and synthetic compounds, including gold (Au), silver (Ag), cuprite (Cu), galena (Pb), sphalerite (Zn), pyrite (S, Fe), arsenopyrite (As), stibnite (Sb), bismuth selenide (Bi), tellurium (Te). Matrix effects were corrected using the ZAF software provided by JEOL.

dendritic beresitization along fissures, and then to sparsely disseminated pyritization. The granite turns from grayish-white to black-gray to shallow flesh pink; the rock type transitions from beresite to monzonitic granitic cataclasite to granitic porphyroclastic rock to cataclastic adamellite; and the rock texture moves from porphyroclastic to granulitic to crushed-powdered to blastogranitic (Fig. 5).

The ZK01 deep borehole intersects various alteration types. The corresponding details are as follows. (1) Potassic alteration appears within the fault alteration zone, having an off-shallow flesh-pink color and vein-like and lumpy characteristics. This alteration occurs as unevenly distributed K-feldspar, replacing plagioclase, while the quartz in the granite and biotite has been replaced by sericite, yielding pseudomorphism. The plagioclase has been widely replaced by K-feldspar and has formed detached island residues (Figs. 5a, b). (2) Silification: The altered rock is off-grayish white in color and occurs as veins, stockworks, and lumps. The early-stage silicified quartz has been deformed under late-stage stress and exhibits wavy and banded extinctions. The late-stage silicified quartz mostly occurs as grains or subhedral columns, with a high automorphism degree. (3) Pyritization: The pyrite occurs as veinlets, stockworks, and disseminations filling the granite fissures (Fig. 5a). (4) Sericitization: This alteration is off-grayish white to shallow-gray to grayish-green in color. The granite has been transformed into sericite and quartz following hydrothermal activity. The sericite occurs as fine flakes and has typically developed along with feldspar. Quartz appears in the form of anhedral grains or subhedral columns. The sericite and quartz are mostly the products of feldspar alteration, with quartz of hydrothermal origin appearing. The biotite and hornblende in the protolith tend to have disappeared via decomposition. (5) Beresitization: This is the main alteration type of the mineralization stage, which mainly occurred through interaction between water-rich hydrothermal fluids, S, SiO_2, NaCl, and granite. This alteration type is closely correlated with the gold mineralization formation, time, and spatial distribution. Generally, this alteration has an off black-gray to shallow-green color. The main mineral associations are pyrite, sericite, and quartz. The pyrite usually occurs in a disseminated, veinlet-stockwork, or lumpy configuration. The sericite is micro-flaky and the quartz occurs as anhedral grains or columns (Figs. 5b−f). (6) Chloritization: This alteration exhibits an off-dark green color and results from hornblende or biotite chloritization. (7) Carbonatization: This is the main alteration type associated with hydrothermal activity and the late mineralization stage, and is expressed as veinlets and stockworks that are mainly composed of calcite and ankerite. This alteration type is commonly associated with quartz and

Table 4. Alteration zoning of the deep part of Jiaojia Fault.

Sequence number	Depth range/m	Zone name	Main characteristics	Mineralization
1	2416.29−2466.44	Weakly beresitized cataclastic adamellite	Essentially exhibits granite characteristics with weak beresitization; pyrite veinlets fill fissures or pyrite is sparsely disseminated	Gold mineralized layer
2	2466.44−2549.59	Beresitized granitic cataclasite	Weak beresitization and intense sericitization and carbonatization	Gold mineralized layer/horizon
3	2549.59−2801.34	Beresitized granitic cataclastic adamellite	Shallow grayish-white to shallow flesh pink in color, with blastogranitic and cataclastic structures and dendritic or stockworked beresite veins filling the fissures	Gold mineralized layer and secondary gold ore layer
4	2801.34−2801.58	Fault gouge and tectonic breccia		
5	2801.58−2810.89	Sericite-carbonate vein	Fresh-green, lepidogranoblastic texture, and massive structure, with Cr-bearing sericite	
6	2810.89−2824.39	Beresitized cataclastic biotite-adamellite	Shallow flesh pink to shallow grayish green, with blastogranitic and cataclastic structures, with pyrite veinlets crosscutting along fissures	Secondary gold ore layer
7	2824.39−2854.59	Beresite and beresitized granitic porphyroclastic, granulitic, and crushed-powdered rocks	Gray-black, mylonitic, and cataclastic structures, where the most intensive fracturing alteration and mineralization are apparent	Main gold ore layer
8	2854.59−2854.69	Black fault gouge	Dark-black shallow green, loose in structure	
9	2854.69−2876.89	Beresitized mylonitized granitic cataclasite and beresitized granitic granulitic rock	Shallow flesh pink to dark gray, with mylonitic and cataclastic structures; grayish-black stockworked quartz-pyrite veins and beresitized veinlets crosscutting is apparent	Secondary gold ore layer
10	2876.89−2965.79	Beresitized cataclastic adamellite intercalated with beresitized granitic porphyroclastic rock	Shallow flesh pink, blastogranitic, and cataclastic structures, usually crosscut by veinlet-like or dendritic beresite veins, with weak beresitization.	Gold mineralized layer
11	2965.79−3111.93	Beresitized granitic porphyroclastic and granulitic rocks with local beresite	Shallow gray to shallow flesh pink to dark gray, porphyroclastic, granulitic, and crushed-powdered structures, with intense beresitization	Gold mineralized layer
12	3111.93−3234.16	Weakly beresitized cataclastic biotite-adamellite	Shallow grayish white to shallow gray, with cataclastic texture; pyrite occurs along fissures and the fracturing alteration is weakened	Barren

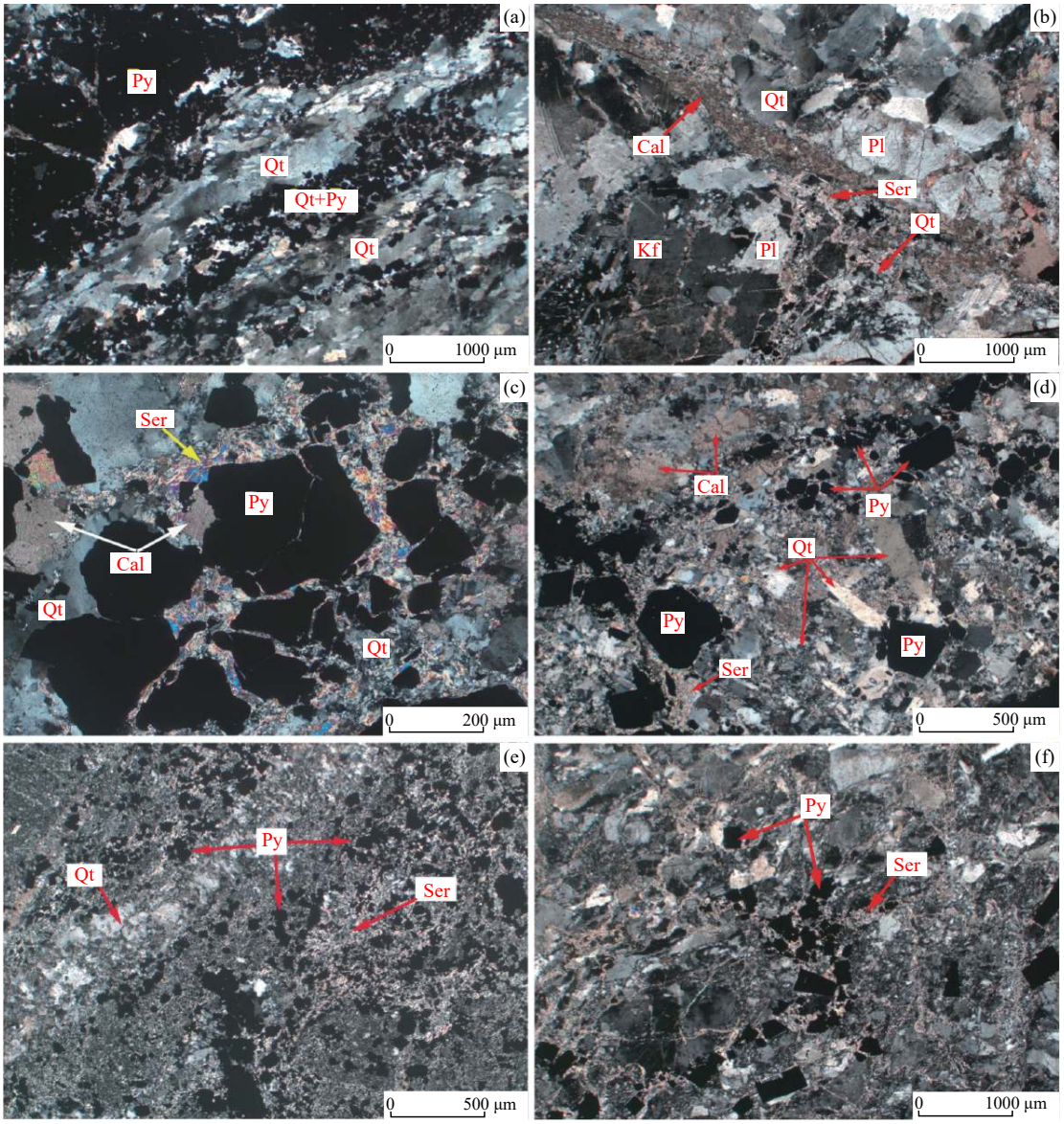

Fig. 5. Microphotographs showing alteration types. a –pyritization and silification; the quartz is elongated and exhibits sub-granulation via-ductile deformation. Quartz-pyrite veins occur along fissures; b–three successive stages of alteration are apparent, i.e., potash alteration with plagioclase replaced by K-feldspar forming residues; networked beresitization; and late-stage carbonate veins cutting through beresite veins; c–beresitization, where pyrite was formed at an early-stage and filled by gold-bearing beresite veins and carbonate veins after fracturing; d–beresitization, where pyrite was formed at a relatively early-stage. Columnar quartz is observable and was carbonatized in the late-stage; e–beresitized cataclasite-type ore (granulitic rock), multi-phased alteration, early-stage beresitization, and late-stage carbonatization; f–beresitized cataclasitetype ore, with beresite veinlets cutting along the rock fissures. Py–pyrite; Qt–Quartz; Ser–Sericite; Cal–Carbonate minerals; Kf–K-feldspar; Pl–Plagioclase (all photographs were taken under cross-polarized light).

sometimes barite, and exhibits multi-phased activity characteristics (Figs. 5b−d).

5.2. Systematic mineralization characteristics at different depths in the Jiaojia metallogenic belt

Geological and petrographic research indicates that the geological characteristics of the ore bodies in the Jiaojia metallogenic belt share the following similarities in the depth direction: The gold ore (mineralization) layers are hosted in the tectonic alteration zone and the main ore bodies have developed along the main fracture plane of the Jiaojia Fault. The ore bodies are principally hosted in the beresitized cataclasite zone, locally extending into the beresitized granitic cataclasite zone. The more developed the fissures in the ore-hosting wall rocks, the denser the pyrite veinlets and the better the mineralization. Pyrite is the main gold-carrying mineral and the gold enrichment is related to the alteration intensity, generally, the higher the alteration, the better the mineralization. The ore bodies are stratiform, large-veinlike, or lenticular, and their attitudes are generally consistent with that of the main fracture plane. The ore bodies mostly exhibit divergence and convergence or swelling and shrinkage characteristics and have stable or relatively stable thicknesses, with evenly or relatively evenly distributed useful

components. Further, thickness and grade are positively correlated. The metal sulfides are mostly disseminated, veinlet-like, stockwork, or veinlet-disseminated. The geological characteristics of the ore bodies at different depths have the following differences: Shallow ore bodies are located below the main fracture plane and minor deep ore bodies are above the plane; the ore-body dip angle decreases in the depth direction; the ore body scale and thickness tend to first increase, with a maximum occurring between −900 m and −2030 m elevation, and then decrease with a tendency towards stability in the depth direction; the gold grade of the ore tends to decrease. The different characteristics of gold minerals at different depths (Table 5) show that the gold-carrier mineral types have dominantly shifted from electrum to native gold with increasing depth. Besides, the gold fineness values are positively correlated with mineralization temperatures. The grain size tends to decrease but varies weakly, with fine grains and micro grains dominating. However, the gold mineral configuration does not change, being dominated by brecciated rock. The gold-mineral occurrence state transitions from intracrystalline gold and fissure gold to intracrystalline gold.

5.3. Mineralization stage

According to the ore mineral composition, mineral paragenetic association, mineral cross-cutting relation, and ore texture structure, the deep gold mineralization alteration of ZK01 can be divided into four stages (Table 6): (1) Quartz-pyrite, (2) gold-beresitization, (3) gold-quartz-polymetallic sulfide, and (4) quartz-barite-carbonate mineral stages. In the quartz-pyrite stage, the main mineral association involves quartz, pyrite, and minor sericite. In the gold-beresitization stage, the main mineral association involves pyrite, sericite, quartz, native gold, and bismuth and tellurium minerals. In gold-quartz-polymetallic sulfide stage, the main mineral association involves pyrite, sericite, quartz, galena, chalcopyrite, and electrum, with native bismuth in some samples. The quartz-barite-carbonate mineral stage is dominated by quartz and carbonate minerals, with local barite. The mineralization stages are similar to those in the shallow part (Jiang XH et al., 2011); however, in the deep part, the alteration range is larger, the beresitization is more intense, and the quartz and sericite grains are finer and more closely intergrown. This may yield low Si content, high K content, and fast crystallization of hydrothermal fluids. In fact, the gold-beresitization stage also exhibits multi-phased activity, which is expressed in the form of superimposition and composition of multiple mineralization stages. This phenomenon is also observable in the central shallow part of the gold belt (Yang LQ et al., 2016).

Table 5. Comparison of geological and gold mineral characteristics of ore bodies in Jiaojia metallogenic belt at different depths.

Deposit name	Deep Sizhuang	Deep Jiaojia	Deep Shaling	Zhaoxian	Wuyi Village
Orebody No.	Ⅲ-2	Ⅰ	Ⅰ-2	Ⅰ-2	Ⅰ-3
Occurrence elevation/m	–235– –760	–500– –1080	–940– –2030	–1836– –2130	–2806– –2812
Orebody dipping /(°)	SW or NW	NW	243–291	242–280	272
Orebody dip angle /(°)	26–45	16–30	6–42	13–27	20
Ore body thickness /m	1.18–8.58, average: 3.46	0.91–37.82, average: 10.95	1.20–125.64, average: 14.63	1.40–13.83, average: 7.73	5.00
Ore body grade /10^{-6}	1.52–17.20, average: 7.10	1.01–11.97, average: 3.74	1.00–11.37, average: 3.09	0.10–18.40, average: 3.53	0.08–13.65, average: 3.13
Gold mineral species	Dominated by electrum with secondary kustelite	Dominated by native gold with minor electrum	Dominated by native gold with extremely minor electrum		Dominated by native gold with secondary electrum
Gold mineral fineness/‰	295–776 average: 532.25	777–848			771–909
Gold mineral shape	Dominantly brecciated, wheat-grained, dendritic, round, secondarily grained, needle-like, with minor flakiness	Dominantly grained, with minor dendritic, flaky, and needle-like characteristics	Dominantly brecciated, secondarily flaky, and wheat grained; with minor dendritic, round, and needle-like characteristics		Dominantly brecciated, secondarily flaky, and wheat grained; with minor dendritic, round, and needle-like characteristics
Gold mineral grain size	Dominantly micro-grained, secondarily fine-grained, with minor medium-grained characteristics	Dominantly fine- and micro-grained, with minor medium-grained characteristics	Dominantly fine-grained, secondarily micro- and medium-grained, with minor coarse-grained characteristics		Dominantly fine- and micro-grained, secondarily medium-grained
Gold mineral occurrence state	Dominantly inter-crystalline gold and fissure gold with minor inclusion gold		Dominantly intracrystalline gold and secondarily inclusion gold with minor fissure gold		Dominantly intracrystalline gold and secondarily fissure gold with minor inclusion gold
Reference	Yang ZL et al., 2007	Song MC et al., 2010	Song MC et al., 2017	Zhu DC et al., 2018	This paper

Table 6. Gold mineralization stages and mineral growth sequence of deep part of the Jiaojia metallogenic belt.

Mineralization stages	I	II	III	IV
	Quartz-pyrite stage	Gold-beresitization stage	Gold-quartz-polymetallic sulfide stage	Quartz-barite-carbonate mineral stage
Pyrite	———	———	———	
Quartz	———	———	———	———
Minor Sericite	——	———	———	
Pyrrhotite			——	
Galena			———	
Sphalerite			———	
Chalcopyrite			———	
Tetrahedrite			——	
Telluric Bismuth		—		
Tetradymite		—		
Native Gold		———	———	
Electrum		—	———	
Native Bismuth			——	
Chlorite		——		
Clay Mineral		———	———	
Carbonate Mineral		—	——	———
Barite				—

6. Discussion

6.1. The significant potential of Jiaojia Fault Belt for deep gold mineralization prospecting

The Jiaojia Fault Belt has been recognized as China ’s largest gold belt in terms of gold resources/reserves and has significant potential about deep gold mineralization prospecting. In the 1970s, the discovery of an ultra-large “Jiaojia-type” gold deposit resulted in dramatic breakthroughs in gold metallogenic theory. As one of the most significant gold belts of northwestern Jiaodong, continuous breakthroughs have been made through prospecting of the deep second mineralization enrichment zone of the Jiaojia metallogenic belt over the past several years. These findings have identified Jiaojia as a Kilton giant gold deposit with 1400 t measured gold resources at a depth exceeding 2000 m. In this study, ZK01 has been successfully used to define the alteration and mineralization characteristics of the Jiaojia metallogenic belt at 3000 m depth. Note that this belt turns with a gentle dip at this depth. In addition, data gathered via ZK01 have been successfully analyzed to define the Jiaojia metallogenic belt at a depth interval of 2416.29 m to 3234.16 m. The thickness of the alteration zone is up to 817.87 m, and six new layers of gold ore bodies have been discovered. The accumulative ore intersection thickness is 20.87 m and the average gold grade is 1.85×10^{-6} gold, while the industrial ore body is 5.85 m thick with average and maximum grades of 3.14×10^{-6} and 13.65×10^{-6} gold, respectively. This drillhole has effectively verified the resource potential of the Jiaodong gold deposits at a 3000 m depth and is recognized as the first drillhole with intersected hard-rock gold mineralization in China. Previous research has indicated that, at a depth interval of 2000 m to 4000 m in the Wuyi Village area, there are 912 t of inferred gold resources, while the entire Jiaodong area has about 4000 t of inferred gold resources at a depth interval of 2000 m to 4000 m, based on the data gathered from the deep drillhole (Yu XF et al., 2015). To summarize, the ZK01 ultra-deep scientific drillhole has facilitated significant breakthroughs with regard to deep prospecting of the Jiaojia metallogenic belt, revealing the considerable resource potential and prospects of this belt at an along-hole depth of 7000 m and a vertical depth of 3000 m.

6.2. Relationships between dark gouge of the main fracture plane and gold ore body occurrence spaces of Jiaojia Fault Belt

Previous massive geological exploration revealed that the main ore bodies in the Jiaojia metallogenic belt are mainly hosted in two mineralized alteration zones, i.e., the beresite and beresitized granitic cataclasite near the footwall of the Jiaojia main fault. Through isotopic testing, Song MC et al. (2010, 2012) determined the isotope age of the Jiaojia fault gouge, which was in the range of 131.05–123.53 Ma. Those researchers also argued that the gouge in the main fracture plane is a favorable impermeable layer, constituting the ore-forming fluid trap layer and causing accumulation of ore-forming materials below the trap layer; thus, they believed that the gold ore bodies are mainly distributed in the footwall of the Jiaojia Fault. In addition, Zhang C (2015) performed a detailed compositional analysis using X-ray powder-diffraction, and revealed that the main composition corresponds to quartz, feldspar, other granite residues, hydrothermally altered illite, smectite, kaolinite, and chlorite minerals, and hydrothermal minerals such as dolomite, calcite, pyrite, and quartz. The fault gouge exists at two locations in the deep Jiaojia Fault Belt and was mainly formed through post-mineralization faulting. The main fracture plane of the mineralization stage may have been covered by

mineralization. The findings of the present study indicate that the deep-seated ore bodies differ from the shallow bodies of the Jiaojia Fault Belt, that is, the former have principally developed above the main fracture plane, whereas the shallow ore bodies (at an elevation exceeding −1556 m) are typically characterized by their location below the main fracture plane. This result suggests that the previous understanding that ore-forming fluids enriched the area below the main fracture plane because of blocking by the fault gouge is limited. Besides, the shallow ore bodies of the Jiaojia metallogenic belt are mainly hosted inside Mesozoic granites or near the contact between granite and Early Pre-Cambrian metamorphic rock series. In contrast, all deep-seated ore bodies occur inside the ore-controlling fault alteration zone inside the Mesozoic granites. Accordingly, the authors assume that the fault gouge is not a key factor controlling ore body emplacement during mineralization. This new knowledge is of great significance for the development of accurate ore prospecting models and determination of favorable positions for deep prospecting, metallogenic prognosis, and resource potential evaluation.

6.3. Comparison of mineralized alteration zoning characteristics between shallow and deep parts of Jiaojia metallogenic belt and controlling factors

ZK01 has revealed that the Jiaojia Fault Belt tends to dip gently in the depth direction, dipping at about 25° and about 20° at depths of 2000 m and 2850 m, respectively. The fracturing, alteration and mineralization, and tectonic type differ between the shallow and deep parts of the Jiaojia metallogenic belt. The deep part displays typical zoning from the interior to exterior, which generally consists of cataclastic granite, granite cataclasite, weakly beresitized granitic cataclasite, beresitized cataclasite, and fault gouge (zones). The various zones are usually in a relationship of gradual transition or occur alternately or repeatedly. According to the data obtained from the deep drillhole, in the deep part of the Jiaojia metallogenic belt, beresite has only developed at the highest-intensity fracturing alteration position. This rock extends discontinuously and usually occurs as strips and lenses. The main mineralized alteration mechanisms include silification, pyritization, sericitization, beresitization, chloritization, carbonatization, and biotitization. Beresitization is most closely related to mineralization. Gold beresitization is the main mineralization stage, superimposed with the quartz-pyrite stage. The gold-quartz-polymetallic sulfide stage has not developed, and the late-stage corresponds to the quartz-barite carbonate stage. Compared to the shallow part, the deep part has gold ore bodies at lower grades and orebody thicknesses, but more intense silification. These characteristics indicate that the ore-forming element Si began to precipitate first, followed by gold precipitation. Note that Si precipitation indicates changes in physical and chemical conditions [T, P, $f_{(O_2)}$, pH, and other hydrothermal fluid chemical properties]. As previously reported, gold in hydrothermal gold deposits is generally transported in complex compounds such as $AuCl^{-2}$ and gold $(HS)^{-2}$ (Henley RW, 1973; Kyle PR and Seward D, 1984; Seward D and Tulloch AJ, 1991; Phillips RE et al., 2014). It is therefore inferred that, during mineralization with ore-forming fluids migrating toward the deep fractured zone of the Jiaojia Fault Belt, boiling due to decreasing ore-hosting tectonic pressure decreased the ore-forming fluid temperature. The temperature decline then induced the precipitation of massive quartz and may reduce the solubility of gold complexes in the residual fluids. The Si content gradually decreased while the fluid rose, the gold precipitated, and a further large-scale gold mineralization event occurred. This controlling factor may have been the main contributor to the intense silification and quartz-vein-type ore bodies that developed across the gold deposits in northwestern Jiaodong (Wei Q et al., 2015; Fan HR et al., 2016).

7. Conclusions

Based on data obtained via deep drillhole ZK01, this paper reported the deep geological mineralization characteristics of the Jiaojia metallogenic belt at 3000 m depth, along with their implications. The main findings can be summarized as follows.

(i) The creation of ZK01 facilitated significant breakthroughs concerning deep prospecting of the Jiaojia metallogenic belt. Notably, this is China's first drillhole with intersected hard-rock gold mineralization. Hence, the alteration and mineralization characteristics of the Jiaojia metallogenic belt at 3000 m depth were determined (the Jiaojia metallogenic belt dips more gently at 3000 m). In particular, the ZK01 borehole allowed successful characterization of the Jiaojia metallogenic belt at a depth interval of 2416.29 m to 3234.16 m. The alteration zone was found to be up to 817.87 m thick and six layers of gold ore bodies were discovered. The accumulative ore intersection thickness was determined to be 20.87 m and the average gold grade was determined to be 1.85×10^{-6} gold. The industrial orebody was found to be 5.85 m thick with average and maximum gold grades of 3.14 $\times10^{-6}$ and 13.65×10^{-6} gold, respectively. Also, seven layers of mineralized orebodies were delineated in the deep part of the Jiaojia metallogenic belt (0.5×10^{-6} to 1.0×10^{-6} gold), having a total apparent thickness of 11 m. Moreover, the analysis of samples from this borehole effectively verified the resource potential of the Jiaodong gold deposits at 3000 m depth. The results of the present study indicate that the Wuyi Village prediction area contains 912 t of inferred gold resources at a depth interval of 2000−4000 m and that the entire Jiaodong area has about 4000 t of inferred resources at a depth interval of 2000−4000 m based on the samples collected from the deep hole.

(ii) Analysis of ZK01 data has also revealed that the Jiaojia Fault Belt tends to dip gently in the depth direction, with dip angles of about 25° and about 20° at vertical depths of 2000 m and 3000 m, respectively. The fracturing, alteration and mineralization, and tectonic type differ between the shallow and deep parts of the Jiaojia metallogenic belt. The deep part exhibits typical zoning from the interior to the exterior generally consisting of cataclastic granite, granite cataclasite, weakly beresitized granitic cataclasite, beresitized

cataclasite, and fault gouge (zones). The relationships between the various zones are in gradual transition or occur alternately and repeatedly. From the ZK01 intersection, the beresite of the deep part of the Jiaojia metallogenic belt has only developed at the position corresponding to the most intense fracturing alteration. Further, this rock extends discontinuously and usually occurs as strips and lenses.

(iii) Data obtained from ZK01 also indicate that the pyritized cataclastic granite-type ore in the deep part of the Jiaojia metallogenic belt has a mineralization intensity closely related to the degree of pyrite vein development; the higher the pyrite content, the wider the veins and the higher the gold grade. The deep gold ore has higher gold fineness than the shallow ore and contains joseite, tetradymite, and native bismuth, indicating a higher deep gold mineralization temperature and the presence of mantle-sourced material possibly involved in the mineralization.

(iv) Finally, analysis of ZK01 data has revealed that the deep-seated orebodies are mainly located above the main fracture plane (fault gouge), which contradicts the previous understanding that the fault gouge blocked hydrothermal activity during mineralization and that the orebodies are located below the main fracture plane. Previous research has indicated that the shallow orebodies are typically hosted in the contact zone between the Linglong Granite and Jiaodong Group or meta-gabbro; however, the deep-seated orebodies are hosted far from this contact zone and within the Linglong Granite zone. This new knowledge is of great significance for the development of accurate prospecting models and the determination of favorable positions for deep prospecting, metallogenic prognosis, and resource potential evaluation.

CRediT authorship contribution statement

Xue-feng Yu and Da-peng Li developed the theoretical formalism, performed the analytic calculations. De-ping Yang, Wei Shan, Yu-Xin Xiong and Nai-jie Chi participated in the whole drilling project. Ke Geng and Peng-fei Wei provided critical feedback and helped shape the research, analysis and manuscript. Peng-rui Liu carried out the thin section identification. All authors discussed the results and contributed to the final manuscript.

Declaration of competing interest

The authors declare no conflict of interest.

Acknowledgment

This study was financially supported by the National Natural Science Foundation of China (41772076, 41672084, 41372086, 41503038), the National Key Research and Development Program of China (2016YFC0600105-04, 2016YFC0600606), the Key Research and Development Program of Shandong Province (2017CXGC1601, 2017CXGC1602, 2017CXGC1603), and the Special Fund for “Taishan Scholars” Project of Shandong Province.

References

Cai YC, Fan HR, Santosh M, Hu FF, Yang KF, Li XH. 2018. Decratonic gold mineralization: Evidence from the Shangzhuang gold deposit, eastern north china craton. Gondwana Research, 54, 1–22. doi: 10.1016/j.gr.2017.09.009.

Chai P, Zhang ZY, Hou ZQ. 2019. Geological and fluid inclusion constraints on gold deposition processes of the Dayingezhuang gold deposit, Jiaodong Peninsula, China. Acta Geologica Sinica (English edition), 93(4), 955–971. doi: 10.1111/1755-6724.13849.

Chen YJ, Pirajno F, Lai Y, Li C. 2004. Metallogenic time and tectonic setting of the Jiaodong gold Province, eastern China. Acta Petrologica Sinica, 20, 907–922 (in Chinese with English abstract).

Deng J, Wang CM, Bagas L, Carranza EJM, Lu YJ. 2015. Cretaceous-Cenozoic tectonic history of the Jiaojia Fault and gold mineralization in the Jiaodong Peninsula, China: Constraints from zircon U-Pb, illite K-Ar, and apatite fission track thermochronometry. Mineralium Deposita, 50, 987–1006. doi: 10.1007/s00126-015-0584-1.

Deng J, Xu SL, Fang Y, Zhou XQ, Wan L. 1996. Tectonic system and metallogenic dynamics in northwestern Jiaodong. Beijing, Geological Publishing House, 1 –98 (in Chinese with English abstract).

Deng J, Yang LQ, Ge LS, Wang QF, Zhang J, Gao BF, Zhou YH, Jiang SQ. 2006. Study on the Structural System of Jiaodong mining concentration Area. Progress in Natural Science, 16, 513–517.

Ding ZJ, Sun FY, Li GH, Ji P, Kong Y. 2015. Accurate zircon U-Pb dating of Early Yanshanian molybdenum-tungsten mother rocks in Xingjiashan area of Jiaodong Peninsula and its significance. Geology in China, 42(2), 556–569 (in Chinese with English abstract).

Dou JZ, Zhang HF, Tong Y, Wang F, Chen FK, Li SR. 2018. Application of geothermo-barometers to mesozoic granitoids in the Jiaodong Peninsula, eastern China: Criteria for selecting methods of pressure estimation and implications for crustal exhumation. Journal of Asian Earth Sciences, 160, 271–286. doi: 10.1016/j.jseaes.2018.01.019.

Editorial Department of China Geology. 2018. China has launched a deep gold prospecting demonstration project to evaluate gold resource potential within 3000 m underground in the east of the North China Craton. China Geology, 1, 572–573. doi: 10.31035/cg2018047.

Fan HR, Feng K, Li XH, Hu FF, Yang KF. 2016. Mesozoic gold mineralization in the Jiaodong and Korean peninsulas. Acta Petrologica Sinica, 10, 3225–3238 (in Chinese with English abstract).

Fan HR, Hu FF, Yang JH, Shen K, Zhai MG. 2005. Fluid evolution and large-scale gold metallogeny during Mesozoic tectonic transition in the eastern Shandong Province. Acta Petrologica Sinica, 21, 1317–1328 (in Chinese with English abstract).

Goldfarb RJ, Groves DI, Gardoll S. 2001. Orogenic gold and geologic time: A global synthesis. Ore Geology Reviews, 18, 1–75. doi: 10.1016/S0169-1368(01)00016-6.

Goldfarb RJ, Santosh M. 2014. The dilemma of the Jiaodong gold deposits: Are they unique? Geoscience Frontiers, 5, 139–153. doi: 10.1016/j.gsf.2013.11.001.

Goldfarb RJ, Taylor RD, Collins GS, Goryachev NA, Orlandini OF. 2014. Phanerozoic continental growth and gold metallogeny of Asia. Gondwana Research, 25, 48–102. doi: 10.1016/j.gr.2013.03.002.

Groves DI, Goldfarb RJ, Gebre-Mariam M, Hagemann SG, Robert F. 1998. Orogenic gold deposits: A proposed classification in the context of their crustal distribution and relationship to other gold deposit types. Ore Geology Reviews, 13, 7–27. doi: 10.1016/S0169-1368(97)00012-7.

Guo LN, Marsh E, Goldfarb RJ, Wang ZL, Li RH, Chen BH, Li JL. 2016. A comparison of Jiaojia- and Linglong-type gold deposit ore-

forming fluids: Do they differ? Ore Geology Reviews, 88, 511–533. doi: 10.1016/j.oregeorev.2016.12.003.

Han ZY, Yu XW, Li SJ, Tian JX, Wang ZL, Yu XJ, Wang LG. 2019. He-Ar isotopic tracing of pyrite from ore-forming fluids of the Sanshandao Au deposit, Jiaodong Area. Acta Geologica Sinica (English edition), 93(6), 1797–1807. doi: 10.1111/1755-6724.14335.

Hao ZG, Fei HC, Hao QQ, Liu L. 2016. Two super-large gold deposits have been discovered in Jiaodong Peninsula of China. Acta Geologica Sinica (English edition), 90(1), 368–369. doi: 10.1111/1755-6724.12660.

Henley RW. 1973. Solubility of gold in hydrothermal chloride solutions. Chemical Geology, 11, 73–87. doi: 10.1016/0009-2541(73)90044-2.

Hou ML, Jiang YH, Jiang SY, Ling HF, Zhao KD. 2007. Contrasting origins of late Mesozoic adakitic granitoids from the northwestern Jiaodong Peninsula, East China: Implications for crustal thickening to delamination. Geological Magazine, 144, 619–631. doi: 10.1017/S0016756807003494.

Jiang SY, Dai BZ, Jiang YH, Zhao HX, Hou ML. 2009. Jiaodong and Xiaoqinling: Two orogenic gold provinces formed in different tectonic settings. Acta Petrologica Sinica, 25, 2727–2738 (in Chinese with English abstract).

Jiang XH, Fan HR, Hu FF, Yang KF, Lan TG, Zheng XL, Jin NX. 2011. Comparative studies on fluid inclusionin different depths and oregenesis of the Sanshandao gold deposit, Jiaodong Peninsula. Acta Petrologica Sinica, 27, 1327–1347 (in Chinese with English abstract).

Kerrich R, Goldfarb RJ, Groves, DI, Steven G, Jia YF. 2000. The characteristics, origins, and geodynamic settings of supergiant gold metallogenic provinces. Science in China (Series D), 43, 1–68.

Kyle PR, Seward D. 1984. Dispersed rhyolitic tephra from New Zealand in deep-sea sediments of the Southern Ocean. Geology, 12, 487–490. doi: 10.1130/0091-7613(1984)12<487:DRTFNZ>2.0.CO;2.

Li HM, Shen YC, Liu TB. 2002. Genetic relationship between Jiaojia-type and Linglong-type gold deposits in northwesrern Jiaodong district, Shandong Province. Mineral Deposits, 21, 621–624 (in Chinese with English abstract).

Li J, Song MC, Li SY, Zhou XJ, Song YX, Ding ZJ, Yang LX, Wang SS, Jiang F, Li Q. 2016. Geological and geochemical features of the Dadengge gold polymetallic deposit in Jiaodong Peninsula. Geology in China, 43(1), 221–237 (in Chinese with English abstract).

Li J, Song MC, Liang JL, Jiang MY, Li SY, Ding ZJ, Su F. 2020a. Source of ore-forming fluids of the Jiaojia deeplyseated gold deposit: Evidences from trace elements and sulfur-helium-argon isotopes of pyrite. Acta Petrologica Sinica, 36(1), 297–313 (in Chinese with English abstract). doi: 10.18654/1000-0569/2020.01.23.

Li J, Zhang LP, Li CY, Jiang MY. 2020b. Rb-Sr age of pyrite in Guocheng gold deposit, Jiaodong. Geology in China, http://kns.cnki.net/kcms/detail/11.1167.P.20191204.1000.002.html (in Chinese with English abstract).

Li JJ, Luo ZK, Liu XY, Xu WD, Luo H. 2005. Geodynamic setting for formation of large-superlarge gold deposits and Mesozoic granites in Jiaodong area. Mineral Deposits, 24, 361–372 (in Chinese with English abstract).

Li Q, Song H, Zhang GY, Yan WQ, Nie R, Si F, Yao C, Zhao ZC, Li W. 2019. Why the temperature parameters of mineralization are similar in the Jiaodong gold deposits: An inference from geothermal gradients. Acta Geologica Sinica (English edition), 93(supp.2), 104–105.

Li SR, Santosh M. 2014. Metallogeny and craton destruction: Records from the North China Craton. Ore Geology Reviews, 56, 376–414. doi: 10.1016/j.oregeorev.2013.03.002.

Liu C, Deng JF, Li SR, Xiao QH, Jin TJ, Sun H, Di YJ, Liu Y, Zhao GC. 2018. Discussions on crust-mantle structure during the formation of Yanshanian of large-super large scale deposits in the Jiaodong Gold Ore District: Constraints from ore-forming igneous assemblage. Earth Science Frontiers, 25(6), 296–307 (in Chinese with English abstract). doi: 10.13745/j.esf.sf.2018.11.16.

Liu XD, Deng J, Zhang L, Lin SY, Zhou ML, Song YZ, Xu XL, Lian CQ. 2019. Hydrothermal alteration of the Sizhuang gold deposit, northwestern Jiaodong Peninsula, eastern China. Acta Petrologica Sinica, 35(5), 1551–1565 (in Chinese with English abstract). doi: 10.18654/1000-0569/2019.05.15.

Ma L, Jiang SY, Albrecht WH, Xu YG. 2016. A possible mechanism to thin lithosphere of the North China Craton: Insights from Cretaceous mafic dikes in the Jiaodong pensinsula. Acta Geologica Sinica (English Edition), 90(supp.1), 106–108.

Mao JW, Li HM, Wang YT, Zhang CQ, Wang RT. 2005. The relationship between mantle-derived fluid and gold Ore-formation in the eastern Shandong peninsula: Evidences from D-O-C-S Isotopes. Acta Geologica Sinica, 79, 839–857 (in Chinese with English abstract).

Mao JW, Wang YT, Li HM, Pirajno F, Zhang CQ, Wang RT. 2008. The relationship of mantle-derived fluids to gold metallogenesis in the Jiaodong Peninsula: Evidences from D-O-C-H isotope systematics. Ore Geology Reviews, 33, 361–381. doi: 10.1016/j.oregeorev.2007.01.003.

Mao XC, Wang MJ, Liu ZK, Chen J, Deng H. 2019. Quantitative analysis of ore-controlling factors based on exploration data of the Dayingezhuang gold deposit in the Jiaodong Peninsula. Earth Science Frontiers, 26(4), 84–93 (in Chinese with English abstract). doi: 10.13745/j.esf.2019.04.010.

Miao LC, Luo ZK, Guan K, Huang JZ. 1997. The evolution of the ore-controlling faults in the Zhaoye gold belt, eastern Shandong Province. Contributions to Geology and Mineral Resources Research, 12, 26–35 (in Chinese with English abstract).

Phillips RE, Powell JA, Hallwachs W, Janzen, DH. 2014. A synopsis of the genus Ethmia Hübner in Costa Rica: Biology, distribution, and description of 22 new species (Lepidoptera, Gelechioidea, Depressariidae, Ethmiinae), with emphasis on the 42 species known from Área de Conservación Guanacaste. Zookeys, 461, 1–86. doi: 10.3897/zookeys.461.8377.

Pirajno F, Santosh M. 2014. Rifting, intraplate magmatism, mineral systems and mantle dynamics in central-east Eurasia: An overview. Ore Geology Reviews, 63, 265–295. doi: 10.1016/j.oregeorev.2014.05.014.

Sai SX, Deng J, Qiu KF, Miggins DP, Zhang L. 2020. Textures of auriferous quartz-sulfide veins and $^{40}Ar/^{39}Ar$ geochronology of the Rushan gold deposit: Implications for processes of ore-fluid infiltration in the eastern Jiaodong gold province, China. Ore Geology Reviews, 117, 1–23. doi: 10.1016/j.oregeorev.2019.103254.

Seward D, Tulloch AJ. 1991. Fission-track analysis of Tertiary uplift history of granitic basement in the Victoria Range, West Coast, New Zealand. New Zealand Journal of Geology and Geophysics, 34, 115–120. doi: 10.1080/00288306.1991.9514448.

Shan W, Yu XF, Xiong YX, Chi NJ, Sun B, Li DP, Ma XD, Sun YQ, Shu L. 2019. Results and prospects of deep exploration in Jiaodong area. Shandong Land and Resources, 35(7), 88–88 (in Chinese with English abstract).

Shenyang Institute of Geology and Mineral Resources. 1988. Collection of Regional Metallogenic Conditions of Main Types of Gold Deposits in China (5. Jiaodong area). Beijing, Geological Publishing House, 1–25 (in Chinese).

Song MC, Cui SX, Zhou ML, Jiang HL, Yuan WH, Wei XF, Lu GX. 2010. The deep oversize gold deposit in the Jiaojia field, Shandong province and its enlightenment for the Jiaojia-type gold deposits. Acta Geologica Sinica, 84, 1349–1358 (in Chinese with English abstract).

Song MC, Wang SS, Yang LX, Li J, Li SY, Ding ZJ. 2017. Metallogenic

epoch of nonferrous metallic and silver deposits in the Jiaodong Peninsula, China and its Geological Significance. Acta Geologica Sinica (English Edition), 91(4), 1305–1325. doi: 10.1111/1755-6724.13363.

Song MC, Yi PH, Xu JX, Cui SX, Shen K, Jiang HL, Yuan WH, Wang HJ. 2012. A step metallo-genetic model for gold deposits in the northwestern Shandong Peninsula. China Science: Earth Science, 55, 940–948 (in Chinese with English abstract). doi: 10.1007/s11430-012-4366-7.

Wang J, Zhu LX, Ma SM, Tang SX, Zhang LL, Zhou WW. 2019. Application of the multi-attribute anomaly model for prospecting potential at depth: A case study of the Haiyu Au deposit in the Jiaodong Gold Province, China. Journal of Geochemical Exploration, 207, 1–24. doi: 10.1016/j.gexplo.2019.106359.

Wang JC, Xia B, Tang JR. 2003. Recognition on some key geological problems of Linglong-Jiaojia ore-concentrated district in Shandong Province. Geotectonica et Metallogenia, 27, 147–151 (in Chinese with English abstract).

Wang JH, Tian JX. 2017. The determination of position of the northern extension of Sanshandao fault toward waters and metallogenic prediction. Acta Geologica Sinica, 91(12), 2771–2780 (in Chinese with English abstract).

Wang LG, Qiu YM, McNaughton NJ, Groves DI, Luo ZK, Huang JZ, Miao LC, Liu YK. 1998. Constraints on crustal evolution and gold metallogeny in the northwestern Jiaodong Peninsula, China, from SHRIMP U-Pb zircon studies of granitoids. Ore Geology Reviews, 13, 275–291. doi: 10.1016/S0169-1368(97)00022-X.

Wei Q, Fan HR, Lan TG, Liu X, Jiang XH, Wen BJ. 2015. Genesis of Sizhuang gold deposit, Jiaodong Peninsula: Evidences from fluid inclusion and quartz solubility modeling. Acta Petrologica Sinica, 31, 1049–062 (in Chinese with English abstract).

Yang JH, Chu MF, Liu W, Zhai MG. 2003. Geochemistry and petrogenesis of Guojialing granodiorites from the northwestern Jiaodong Peninsula, eastern China. Acta Petrologica Sinica, 19, 692–700 (in Chinese with English abstract).

Yang KF, Fan HR, Santosh M, Hu FF, Wilde SA, Lan TG, Lu LN, Liu YS. 2012. Reaction of the Archean lower crust: Implications for zircon geochronology, elemental and Sr-Nd-Hf isotopic geochemistry of Late Mesozoic granitoids from northwestern Jiaodong Terrane, the North China Craton. Lithos, 146 –147, 112–127. doi: 10.1016/j.lithos.2012.04.035.

Yang LQ, Deng J, Guo RP, Guo LN, Wang ZL, Chen BH, Wang XD. 2016. World-class Xincheng gold deposit: An example from the giant Jiaodong gold province. Geoscience Frontiers, 7(3), 419–430. doi: 10.1016/j.gsf.2015.08.006.

Yang LQ, Deng J, Song MC, Yu XF, Wang ZL, Li RH, Wang SR. 2019. Structure control on formation and localization of giant deposits: An example of Jiaodong gold deposits in China. Geotectonica et Metallogenia, 43(3), 431–446 (in Chinese with English abstract). doi: 10.16539/j.ddgzyckx.2019.03.005.

Yang LQ, Deng J, Wang ZL, Zhang L, Guo LN, Song MC, Zheng XL. 2014. Mesozoic gold metallogenic system of the Jiaodong gold province, eastern China. Acta Petrologica Sinica, 30, 2447–2467 (in Chinese with English abstract).

Yang LQ, Dilek Y, Wang ZL, Weinberg RF, Liu Y. 2018. Late Jurassic, high Ba-Sr Linglong granites in the Jiaodong Peninsula, East China: Lower crustal melting products in the Eastern North China Craton. Geological Magazine, 155(5), 1040–1062. doi: 10.1017/S0016756816001230.

Yang LQ, Guo LN, Wang ZL, Zhao RX, Song MC, Zheng XL. 2017. Timing and mechanism of gold mineralization at the Wang'ershan gold deposit, Jiaodong Peninsula, eastern China. Ore Geology Reviews, 88, 491–510. doi: 10.1016/j.oregeorev.2016.06.027.

Yang QY, Santosh M, Shen JF, Li S. 2013. Juvenile *vs.* recycled crust in NE China: Zircon U–Pb geochronology, Hf isotope and an integrated model for Mesozoic goldmineralization in the Jiaodong Peninsula. Gondwana Research, 25, 1445–1468. doi: 10.1016/j.gr.2013.06.003.

Yang ZL, Zhang X, Jiang HL. 2007. Geological characteristics of Sizhuang gold deposit in Laizhou City of Shandong Province. Shandong Land and Resources, 23(5), 6–10 (in Chinese with English abstract).

Yao XF, Cheng ZZ, Du ZZ. 2019. Zircon U-Pb ages of postore dykes in Xiejiagou gold deposit northwest Jiaodong Peninsula, China and its geological significance. Acta Geologica Sinica (English edition), 93(supp.2), 129.

Yu XF, Li DP, Tian JX, Shan W, Li HK, Yang DP, Zhang SK, Luo WQ, Xiong YX. 2018a. Progress of deep exploration and theoretical innovation of metallogenic of gold deposits in Shandong Province. Shandong Land and Resources, 34, 1–13 (in Chinese with English abstract).

Yu XF, Shan W, Xiong YX, Geng K, Sun YQ, Chi NJ, Guo BK, Li DP, Li HK, Song YX, Yang DP. 2018b. Deep structural framework and genetic analysis of gold concentration areas in the northwestern Jiaodong peninsula, China: A new understanding based on high-resolution reflective seismic survey. Acta Geologica Sinica (English Edition), 92, 1823–1840. doi: 10.1111/1755-6724.13679.

Yu XF, Song MC, Li DP, Tian JX, Wang LM. 2016. Breakthroughs and prospect of gold deposits in Shandong Province. Acta Geologica Sinica (English Edition), 90, 2847–2862.

Yu XF, Zhang TZ, Wang H. 2015. Shandong Deposit Mineralization Series. Beijing, Geological Publishing House, 1 –644 (in Chinese with English abstract).

Zaw K, Meffre S, Lai CK, Burrett C, Santosh M, Graham I, Manaka T, Salam A, Kamvong T, Cromie P. 2014. Tectonics and metallogeny of mainland Southeast Asia— A review and contribution. Gondwana Research, 26, 5–30. doi: 10.1016/j.gr.2013.10.010.

Zhai MG, Fan HR, Yang JH, Miao LC. 2004. Intra-continental mineralization of the non-orogenic belt type gold deposit – Jiaodong type gold deposit. Earth Science Frontiers, 11, 85–98 (in Chinese with English abstract).

Zhai MG, Santosh M. 2013. Metallogeny of the North China Craton: Link with secular changes in the evolving Earth. Gondwana Research, 24, 275–297. doi: 10.1016/j.gr.2013.02.007.

Zhang C. 2015. Tectonic Ore-control Model of Jiaojia Gold Orefield. Beijing, China University of Geosciences (Beijing), Ph.D. dissertation, 1–55 (in Chinese with English abstract).

Zhao ZL. 2016. Metallogenesis and Prediction of Jiaojia Gold Deposits, Shandong Province. Beijing, Chinese Academy of Geological Science, Master's thesis, 1–63 (in Chinese with English abstract).

Zhu BL, Liu ZJ, Cheng SB, Xue YS, Wang JP, Xu L. 2016. Re-Os isotopic dating of molybdenites from the Yuangezhuang pluton in Jiaodong and its geological significance. Geology in China, 43(4), 1353–1366 (in Chinese with English abstract). doi: 10.12029/gc20160420.

Zhu DC, Zhang W, Wang YP, Tian JX, Liu HD, Hou JH, Gao HL. 2018. Characteristics of ore bodies and prospecting potential of Zhaoxian gold deposit in Laizhou City of Shandong Province. Shandong Land and Resources, 34(9), 14–19 (in Chinese with English abstract).